Subcooled boiling incipience on a highly smooth microheater ☆

Tailian Chen [a,*], James F. Klausner [b], Suresh V. Garimella [a], Jacob N. Chung [b]

[a] School of Mechanical Engineering, Purdue University, West Lafayette, IN 47907-2088, USA
[b] Department of Mechanical and Aerospace Engineering, University of Florida, Gainesville, FL 32611-6300, USA

Abstract

Subcooled boiling incipience on a highly smooth microscale heater ($270\,\mu m \times 270\,\mu m$) submerged in FC-72 liquid is investigated. Using high-speed imaging and a transient heat flux measurement technique, the mechanics of homogeneous nucleation on the heater are elucidated. Bubble incipience on the microheater was observed to be an explosive process. It is found that the superheat limit of boiling liquid is required for bubble incipience. It is concluded that boiling incipience on the microheater is a homogeneous liquid–vapor phase change process. This is in contrast to recent observations of low-superheat heterogeneous nucleation on metallic surfaces of rms roughness ranging from 4 to 28 nm [T.G. Theofanous, J.P. Tu, A.T. Dinh, T.N. Dinh, The boiling crisis phenomenon part I: nucleation and nucleate boiling heat transfer, Exp. Therm. Fluid Sci. 26 (2002) 775–792; Y. Qi, J.F. Klausner, Comparison of gas nucleation and pool boiling site densities, J. Heat Transfer 128 (2005) 13–20; Y. Qi, J.F. Klausner, Heterogeneous nucleation with artificial cavities, J. Heat Transfer 127 (2005) 1189–1196]. Following the explosive bubble incipience, the boiling process on the microheater can be maintained at much lower superheats. This is mainly due to the necking during bubble departure that leaves an embryo from which the next-generation bubbles grow.
© 2006 Elsevier Ltd. All rights reserved.

Keywords: Bubble incipience; Microheater; Homogeneous nucleation

1. Introduction

The commercial success of bubble jet printers [4], among other microscale applications, has inspired many researchers to study the bubble formation mechanism in these microsystems. For such applications, the bubble produced from a microheater should be designed to function in a stable and controllable manner. Therefore, it is important to understand the bubble formation mechanisms on microheaters so that they may be optimally designed and operated. A number of previous studies have investigated the bubble formation mechanism. Iida et al. [5] used a $0.1\,mm \times 0.25\,mm \times 0.25\,\mu m$ platinum film heater subjected to rapid heating (maximum 93×10^6 K/s). The heater temperature was correlated to its electrical resistance. The temperature measured at bubble nucleation suggested the occurrence of homogeneous bubble nucleation in their experiment. Lin et al. [6] used a $50\,\mu m \times 2\,\mu m \times 0.53\,\mu m$ polysilicon resistance heater to produce microbubbles in Fluorinert liquids. Using a computational model and experimental measurements, they concluded that homogeneous nucleation occurs on the microline heater.

Avedisian et al. [7] performed experiments on a heater used in commercial thermal inkjet printers and comprising a mixture of tantalum and aluminum ($64.5\,\mu m \times 64.5\,\mu m \times 0.2\,\mu m$) by applying voltage pulses of short duration. At extremely high heating rates (2.5×10^8 K/s), homogeneous nucleation at the heater surface was suggested as the mechanism for bubble formation, with the nucleation temperature increasing as the heating rate was increased. Zhao et al. [8] used a similar thin-film microheater, $100\,\mu m \times 110\,\mu m$ in size, to investigate the vapor

---

Nomenclature

ΔT_s	superheat limit (K)
$\overline{M}$	molecular weight of FC-72 (g/mol)
J	nucleation rate ($m^{-3}\,s^{-1}$)
J_s	threshold nucleation rate ($m^{-3}\,s^{-1}$)
P_l	bulk liquid pressure (Pa)
P_{sat}	saturation pressure of bulk liquid (Pa)
r_s	threshold vapor embryo radius (m)

R	gas constant of FC-72 vapor
T_l	liquid temperature (°C)
T_e	threshold temperature (°C)

Greek symbols

ρ_l	liquid density (kg/m^3)
σ	surface tension (N/m)

---

explosion phenomenon. They placed the microheater on the underside of a layer of water and the surface temperature of the heater was rapidly raised (about 13×10^6 K/s) by electrical pulses of short duration. By measuring the acoustic emissions using a pressure transducer from an expanding volume of a vapor bubble, the dynamic growth of the vapor microlayer was reconstructed. A maximum pressure inside the vapor volume of 7 bar was calculated from the measured acoustic pressure.

The heating rates in [5–8] were extremely high, and are believed to be important for the homogeneous nucleation process. In contrast, Theofanous et al. [1] observed low-superheat heterogeneous nucleation on a smooth titanium heater with 4 nm rms roughness submerged in water. Qi and Klausner [2,3] also observed low-superheat heterogeneous nucleation more recently on smooth brass (18 nm rms roughness) and stainless steel (28 nm rms roughness) surfaces submerged in ethanol. In contrast, Qi and Klausner [3] observed high-superheat incipience (60 K) on a nano-smooth silicon surface submerged in ethanol. A clear distinction between the required incipience superheat for metallic and non-metallic nano-smooth surfaces was reported. Recently, Balss et al. [9] investigated the effect of surface hydrophobicity on bubble incipience using a pulse-heated microheater and a novel laser strobe microscopy technique. Imaging rates of over 10 million frames/s were achieved. It was found that bubble nucleation requires a higher superheat and occurs at an earlier time for hydrophilic surfaces compared with those that are hydrophobic.

In the present work, bubble incipience on a smooth microscale heater (approximately 10 nm rms roughness) is further investigated. The objective of the work is to establish that bubble incipience under these conditions is indeed a homogeneous process and to elucidate the mechanics of the process. The present experiments have been performed on a resistance heater of size 270 μm × 270 μm, coated with silicon dioxide. A feedback circuit was employed to supply electrical current to the microheater in such a way that the average heater temperature was maintained constant. It should be noted that a constant temperature condition is useful for identifying the nature of boiling incipience because the degree of superheat is a controlling parameter. The incipience process was visualized from the side and the bottom of the semi-transparent

heater, and the transient heat flux of the heater was simultaneously recorded. The time-resolved heat flux was obtained at a speed of over 4000 readings per second, which was greater than twice the imaging frame rate of 2000 frames/s. The flow visualization in side and bottom views and the simultaneous heat flux measurement provide sufficient information to allow a clear identification of the highly transient bubble incipience process.

2. Experimental system

2.1. Microheater

The microheater used for this study is one of 96 individual microheaters laid out in a planar array. Only one heater is active during this investigation. As shown in Fig. 1, the microheater is a serpentine platinum resistance element fabricated on quartz substrate using standard microelec-
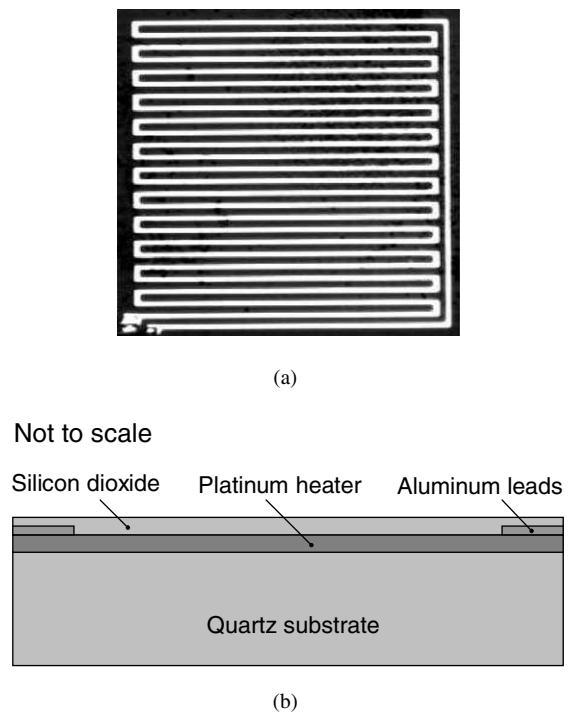

(a)

(b)

Fig. 1. (a) Serpentine filament microheater (270 μm × 270 μm) and (b) a schematic diagram of the fabrication arrangement on quartz substrate.

tronics fabrication techniques. The low thermal conductivity of quartz helps reduce the heat loss from the heater to the quartz substrate and to the ambient. On top of the platinum filament, a very thin layer of silicon dioxide is deposited to protect the heater and form a smooth heating surface (approximately 10 nm rms roughness). The size of the microheater is 270 μm × 270 μm with a thickness of 0.2 μm; its electrical resistance is measured to be 778 Ω at room temperature. An electronic control circuit is used to supply electrical current to the platinum filament to raise the heater temperature to computer-controlled, operator-specified set points. For each set point, the electrical current supplied to the platinum filament is regulated by a feedback loop in the electronic control circuit such that the average heater temperature is maintained constant. Full details of the experimental facility and procedures are available in [10,11].

2.2. Heater temperature control and calibration

The electrical resistance of platinum has a precise linear relationship with temperature. The mechanism for maintaining the heater temperature constant is to maintain a constant electrical resistance via the control circuit shown in Fig. 2. The major components in the temperature control system are a wheatstone bridge and a feedback loop. The feedback loop serves to maintain voltages at V_1 and V_2 equal, such that the wheatstone bridge is balanced. As seen in Fig. 2, the wheatstone bridge consists of metal film resistors (R_1, R_2), a digital potentiometer (R_p), and the microheater (R_h). When the wheatstone bridge is balanced,

$R_1/R_h = R_2/R_p$. The microheater resistance, R_h, is adjusted by varying the digital potentiometer, R_p. The relationship between the heater temperature and the set point of the digital potentiometer is obtained via calibration. An insulated, circulating constant temperature oil bath is heated to a desired calibration temperature within 0.2 °C, and the heater array submerged in the oil bath so that the heater reaches thermal equilibrium with the bath. The set point of the digital potentiometer is increased until the wheatstone bridge is balanced. Thus a one-to-one correspondence between the digital potentiometer setting and heater temperature is established. The heater temperature calibration for different digital potentiometer settings is shown in Fig. 3.

The response frequency of the control system is approximately 15 kHz for the microheater array that consists of 96 microheaters [10]. Because the measurements in this work have a maximum sampling rate of 4 kHz, which is much less than the system response frequency, the heater temperature is maintained constant to good accuracy.

2.3. Experimental conditions

Degassed FC-72 with a saturation temperature of 56 °C is used in all the experiments; the bulk fluid is maintained at one atmosphere and room temperature (25 °C). The experiment setup is shown in Fig. 4. A high-speed digital camera (MotionScope PCI 8000S) is used to capture images at 2000 frames/s with a resolution of 240 × 210 pixels. Visualizations (in side view) are accomplished using a shadow photography technique in which the illumination source
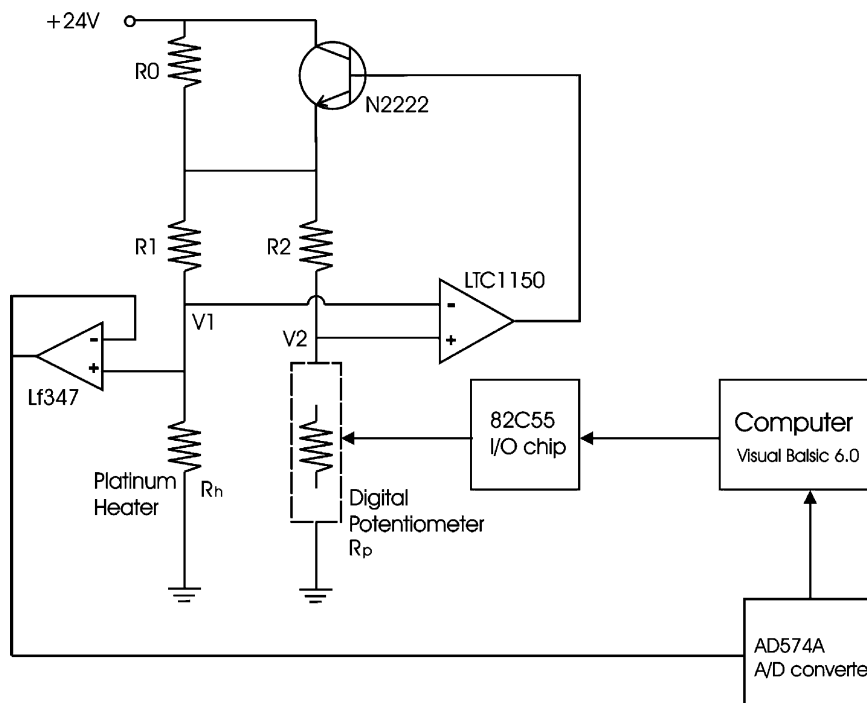

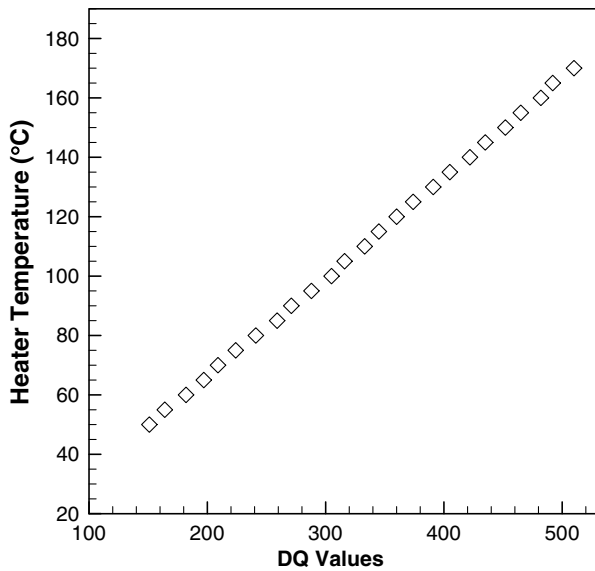Fig. 2. Circuit for heater temperature control.

Fig. 3. Heater temperature calibration for different digital potentiometer set points (DQ values).

(white light in this case) shines on the bubble from the opposite side of the camera using a lens with an effective focal length of 229 mm and an aperture of range *f*/4.5 to *f*/90. The field of view is approximately 0.1 mm. The boiling chamber is fabricated of transparent polycarbonate allowing for the heating surface to be illuminated. Since the object is relatively small and the focal length is large, focusing on the location of bubble incipience can be challenging. A dummy object is placed near the heating surface and the lens focused on this object. Images of good quality that are suitable for analysis are captured by trial and error.

The uncertainties in this experiment include those from the heater temperature and heat flux measurements. The temperature uncertainty is estimated to be ±0.66 °C, while the uncertainty in the measured heat flux is estimated using the method of Kline and McClintock [12] to be ±3.5%.

3. Results and analysis

3.1. Superheat requirement at boiling incipience

The heater temperature is increased by incrementing the set point in the electronic control circuit; the set point can be changed in increments of approximately 0.3 K. Bubble incipience was observed to occur at a heater temperature of 136 °C. When the heater temperature was at 135.7 °C, no incipience was observed. This temperature was maintained for a period of 20 min so that the heater could reach a quasi-steady state with respect to thermal transport into the subcooled bulk liquid. While spatial variations in surface temperature on a single microheater could not be resolved, a simple computational analysis suggests that the maximum variation of absolute temperature on the heater does not exceed 2 °C. With the next step increase in temperature to 136 °C, bubble incipience was observed to occur instantaneously. This procedure was repeated multiple times, and incipience was consistently observed to occur at exactly the same set point corresponding to a 136 °C heater temperature, *i.e.*, a superheat of 80 K. The analysis that follows demonstrates that the observed incipience superheat is approximately the same as the predicted FC-72 superheat limit for homogeneous bubble incipience.
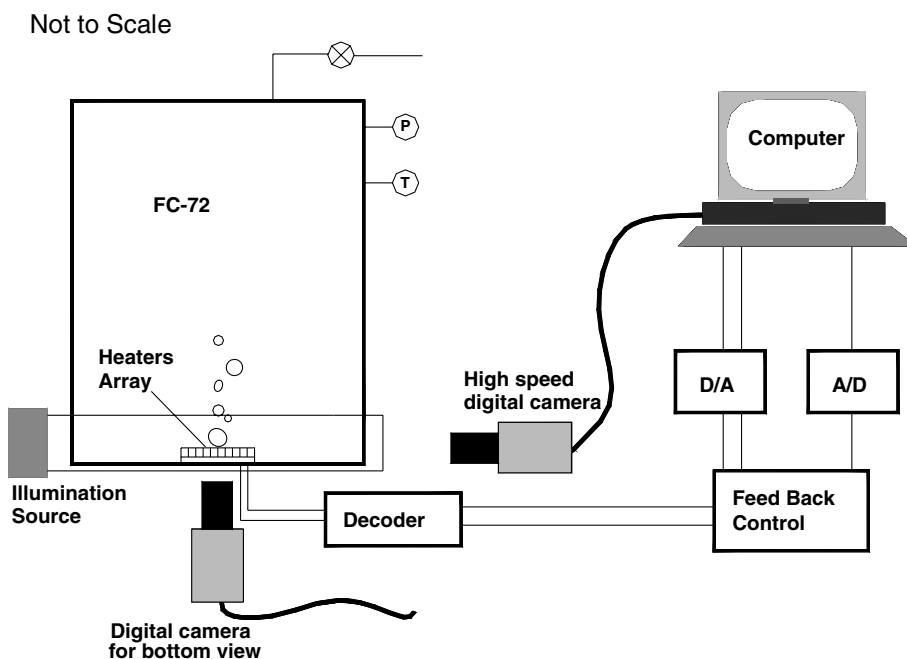

Fig. 4. Schematic diagram of the experimental setup.

3.2. Theoretical basis of homogeneous boiling incipience

The likelihood of homogeneous nucleation depends on the kinetics of the vapor embryo formation process [13]. A vapor embryo of n vapor molecules continually gains molecules due to evaporation and loses molecules due to condensation at the bubble interface. The difference between the rates of these two processes dictates whether the embryo will increase or decrease in size. As liquid approaches the saturation state, density fluctuations in the liquid may result in localized regions where the molecular density has been lowered to nearly the same value as that observed in the saturated vapor, which gives rise to small embryos of vapor within the liquid. The vapor embryo radius, r, increases with increasing liquid temperature, T_1. As described by Kotake and Glass [14], a threshold embryo radius r_s exists corresponding to a threshold temperature T_e. If $T_1 > T_e$, clusters of vapor molecules will form spontaneously leading to homogeneous nucleation and a rapid change of phase from liquid to vapor. The threshold temperature, T_e, defines the superheat limit, $\Delta T_s = T_e - T_{sat}$. According to kinetic theory, the superheat limit can be determined from the nucleation rate, J, which is the net flux of molecules moving from liquid phase to vapor phase. It is a strong function of liquid temperature, as indicated in the following expression:

$$J = 1.44 \times 10^{40} \left(\frac{\rho_1^2 \sigma}{\overline{M}^3}\right)^{0.5} \exp\left(\frac{-1.213 \times 10^{24} \sigma^3}{T_1[\eta P_{sat}(T_1) - P_1]}\right), \quad (1)$$

in which $\eta = \exp\left(\frac{P_1 - P_{sat}(T_1)}{\rho_1 R T_1}\right)$. It was suggested by Kotake and Glass [14] that the threshold nucleation rate, J_s, corresponding to the superheat limit, has a value of 10^{12}. Blander and Katz [15] compared the kinetic limit of superheat for $J_s = 10^{12}$ with experimentally observed superheat limits at atmospheric pressure for a wide range of hydrocarbon liquids and found excellent agreement. In this study, since the boiling liquid is FC-72, an inert perfluorocarbon fluid, and the experiments were performed at 1 atm, it is reasonable to assume a value for J_s of 10^{12}. Table 1 shows calculated values of the nucleation rate of FC-72 at various liquid temperatures and one atmosphere; the temperature

Table 1
Calculation of threshold nucleation rates of FC-72 at 1 atm

T_1 (K)	P_{sat} (kPa)	ρ_1 (kg/m³)	σ (N/m)	J (m⁻³ s⁻¹)
403.2	729.1	1320.9	0.0026	5.26×10^{-24}
404.2	745.0	1311.7	0.0025	1.24×10^{-14}
405.2	761.1	1302.8	0.0025	3.97×10^{-8}
406.2	777.5	1293.9	0.0024	2.26×10^{-2}
407.2	794.1	1284.9	0.0023	2.78×10^{3}
408.2	811.0	1276	0.0023	8.71×10^{7}
409.2	*828.2*	*1267.1*	*0.0022*	*0.81×10^{12}*
409.3	*829.9*	*1266.2*	*0.0022*	*1.90×10^{12}*
410.2	845.7	1258.1	0.0021	4.40×10^{12}
411.2	863.4	1249.2	0.0021	2.55×10^{15}
412.2	881.3	1240.3	0.0020	3.07×10^{18}
413.2	899.6	1232.8	0.0020	1.57×10^{21}

dependence of P_{sat}, σ, and ρ_1 are given in [16] and are included in Appendix A.

As observed in Table 1, the threshold temperature of FC-72, T_s, corresponding to a value of 10^{12} for J_s is 409.2 K (136 °C). This corresponds to a superheat limit of 80 K for FC-72 and is in excellent agreement with the measured incipience wall superheat discussed in Section 3.1. Visualization of the bubble incipience process and the corresponding measured transient heat fluxes are discussed in the following, and shed further light on the homogeneous nucleation process near the heater surface.

3.3. Visualization of boiling incipience

The visualization of boiling incipience in Figs. 5 and 6 reveals the process to be a virtually instantaneous vapor explosion, a physical event in which the volume of the vapor phase increases at a rapid rate. The explosive vapor formation process is usually associated with homogeneous nucleation. Consistent with the observations of Zhao et al. [8], a sound was heard to accompany the bubble incipience process shown in Figs. 5 and 6 indicating that an acoustic pressure wave was produced during the process. The explosive incipience is accompanied by a release of thermal energy from the superheated liquid. During this process, the liquid vaporizes at high pressures and expands almost instantaneously. Fig. 5 shows the side view of the incipience process with an elapsed time of 0.5 m s between consecutive frames. Fig. 6 provides the corresponding bottom view of the incipience process.

The time reference is set to 0 m s at the instant the explosive process starts. Referring to the images at 0 m s in Figs. 5 and 6, the darker shaded regions on the heater surface represent the very initial stage of vapor incipience. The quiescent liquid is disturbed by the vapor expansion pressure field and the incident light aimed at the heater surface is deflected from its original path, resulting in dark blurry regions being recorded by the camera. The first frame in Fig. 6 shows that a vapor phase has not yet formed at this stage.

The images at 0.5 m s clearly show the presence of a vapor phase. Close examination of both the side and bottom views discloses that the vapor expands in all directions on the heater surface, with the bottom image showing the vapor bubble spanning a diameter of approximately three microheaters. It is again emphasized that only the central microheater in the images in Fig. 6 is active. Assuming a hemispherical bubble shape as shown in Fig. 7, the average volumetric vapor expansion rate for this process is roughly estimated to be 82.4 mm³/s. The vapor blanketing of a large area on the heater surface results in low heat transfer rates as will be detailed in the next section. It is interesting to note that Carey and Wemhoff [17] used a thermodynamic analysis to show that when a solid surface is very rapidly heated, homogeneous nucleation could first occur at a location slightly away from the solid surface due to strong wall effects on the liquid molecular motion. However, due to the limited spatial resolution of the imaging
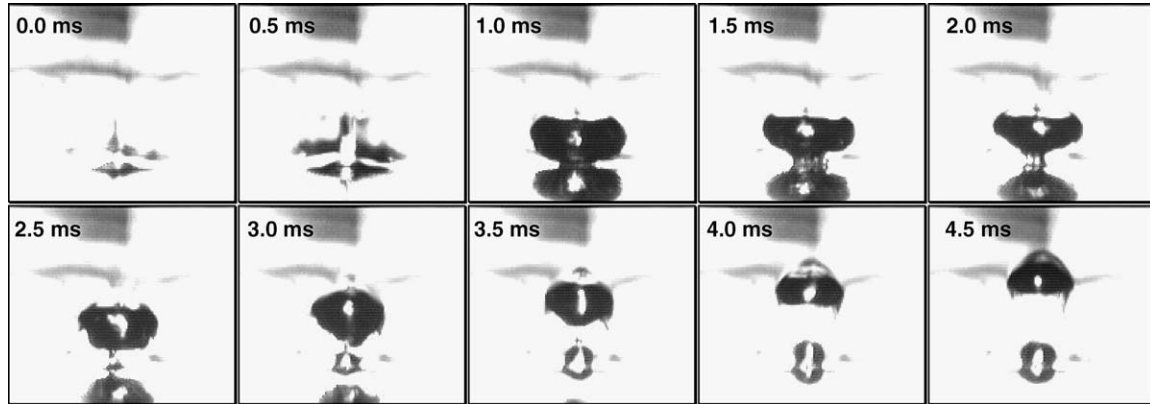
Fig. 5. Side view of progressive stages in the bubble incipience process.
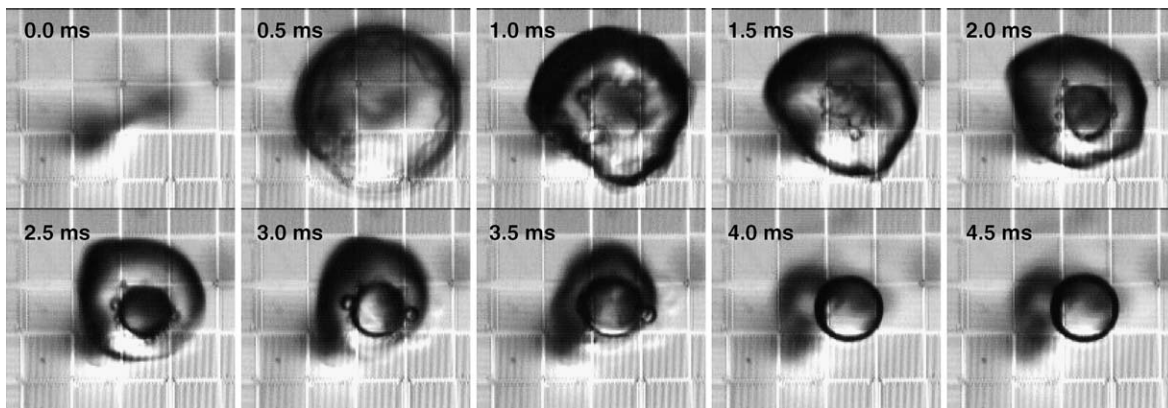

Fig. 6. Bottom view of progressive stages in the bubble incipience process.

system, it is difficult to precisely locate the position of incipience in this study. A mushroom-shaped vapor bubble is seen to take shape in Figs. 5 and 6 by the time 1 m s has elapsed. As the vapor bubble expands rapidly, it pushes on the surrounding liquid. Due to the approximate symmetry of vapor expansion, the net added mass force (referred to as growth force by Thorncroft et al. [18]) pushes the bubble downward and flattens out the bubble dome resulting in a laterally flattened bubble as seen in the images at 1.0, 1.5, 2.0 m s in Fig. 5.
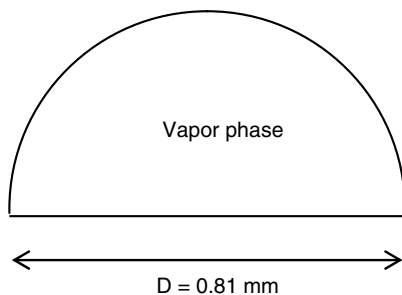

Fig. 7. A simple model for estimating the average vapor expansion rate during the bubble incipience process (vapor bubble has a hemispherical shape with a diameter three times the heater length as observed in the image at 0.5 m s in Fig. 6).

The end stage of vapor expansion is indicated in the images at 1.5 m s in Figs. 5 and 6. At this and succeeding times, the vapor base in contact with the heater surface continues to shrink, and the bubble moves upward. As the first bubble detaches (the image at 2.0 m s in Fig. 5), a new bubble embryo is formed apparently from a small vapor pocket left behind by the departing bubble (2.5 m s in Fig. 5). This embryo grows and becomes a second bubble as the first bubble travels upward into the bulk liquid. This process repeats itself on the heater surface and stable single-bubble boiling is thus established on the micro-heater. It is emphasized that a much lower superheat (as low as 44 °C observed in experiments) is sufficient to sustain single-bubble boiling on the microheater. This is mainly due to the fact that bubble nucleation is seeded by the vapor embryo deposited on the heater surface during the necking process, as the bubble lifts off the heater surface [19]. During the time span of 2.0–3.5 m s (Fig. 5), the bubble tends to recoil and attain a more spherical shape as the first bubble travels into the bulk liquid.

3.4. Transient heat flux measurements

Fig. 8(a) shows the time history of heat flux measurements with the boiling incipience process captured. Details
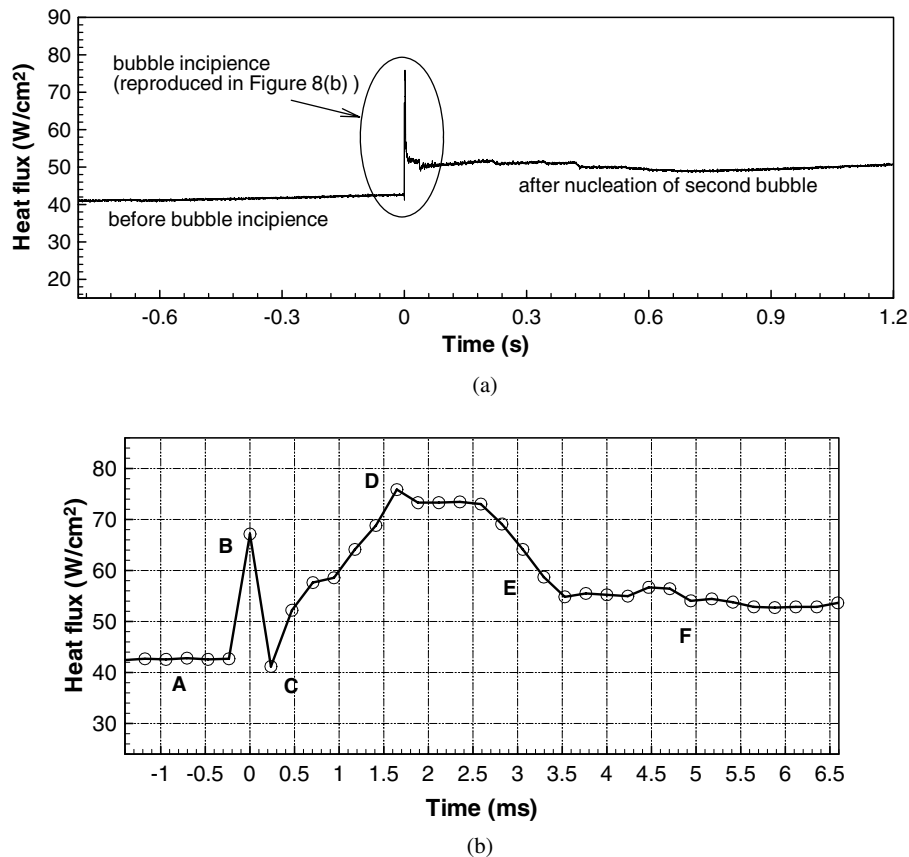
Fig. 8. (a) Heat flux measurement before and after bubble incipience, (b) heat flux measurement during the incipience process.

of the boiling incipience process are shown on a finer time scale in Fig. 8(b). The time scale is synchronized with the images shown in Figs. 5 and 6. The bubble incipience process is associated with a heat flux spike as observed in Fig. 8(a). The heater temperature prior to the bubble incipience (at time zero) is 135.7 °C; the heater temperature following bubble incipience is 136 °C, as described previously. Following the spike, the heat flux settles down to a relatively stable value of roughly 50 W/cm^2, which corresponds to the slow-growth period of the second bubble on the microheater. The details of single-bubble boiling on the microheater are available in [19].

Fig. 8(b) shows details of the transient heat flux variation during bubble incipience. In Fig. 8(b), "A" represents the period of natural convection prior to boiling incipience; "B" corresponds to the very initial stage of vapor expansion, and this point coincides with the images at 0 m s in Figs. 5 and 6. The sudden increase in heat transfer rate at "B" may be attributed to the fact that the heater surface remains well-wetted prior to the vapor expansion event and a large amount of latent heat is consumed from the heater surface to facilitate the phase change process. Point "C" in Fig. 8(b) corresponds to the hemispherical bubble expansion which blankets the heater surface and surroundings with vapor as discussed with the images at 0.5 m s in Figs. 5 and 6. The decreased heat flux at point "C" is attributed

to the blanketing of the heater surface and its surroundings with vapor. The segment from "C" to "D" corresponds to the process when the bubble base in contact with the heater surface starts to shrink as the bubble starts lifting off. The bubble stretches vertically and shrinks laterally as the buoyancy force pulls the bubble away from the heater surface. This results in the contact line being moved towards the center of the heat source, which causes liquid rewetting of the previously vapor-covered area. A second bubble is formed almost instantaneously following the detachment of the first bubble. It appears that a vapor embryo left by the departing bubble on the heater facilitates the formation of the second bubble as described earlier. The formation of the second bubble and its induced heat transfer enhancing effects, such as turbulent mixing on the heater surface, results in the observed enhancement in heat flux during this segment. The heat transfer process around point "D," however, is very complex and is not fully explained by simple qualitative explanations.

The segment from "D" to "E" in Fig. 8(b) corresponds to the period when the second bubble undergoes slow growth prior to departure. The heat flux drops as a result of heater surface dryout. The present work is restricted to heat transfer at the incipient superheat; details of single-bubble boiling heat transfer are described in detail in prior work [19]. It may be noted that below the superheat limit

(80 K for FC-72 at 1 atm), nucleate boiling dominates the heat transfer process and above the superheat limit, homogeneous boiling accompanied by vapor blanketing dominates the heat transfer process.

4. Concluding remarks

The experimental observations and theoretical calculations in this work reveal that subcooled boiling incipience on the smooth microheater (approximately 10 nm rms roughness) is a homogeneous nucleation process where the superheat limit of FC-72 (80 K) has been reached to initiate the vapor incipience process. The vapor expansion process was found to consist of three stages: initial explosive vapor formation, hemispherical bubble expansion, and bubble detachment. The initial explosive vapor formation results in a heat flux spike while the hemispherical bubble expansion causes a drop in heat flux due to extended vapor blanketing over the heater and its vicinity. After incipience, subsequent bubble nucleation is facilitated by a small amount of vapor left from the previous departing bubble. Thus a stable single bubble ebullition process can be sustained on the microheater at a superheat (44 K) much lower than the superheat required for initial incipience.

Acknowledgement

Appendix A

Temperature dependence of FC-72 saturation pressure, liquid density, and surface tension.

$$P_{sat} = 0.37T_1^3 - 320.92T_1^2 + 94094T_1 - 9289664 \text{ [Pa]} \quad (A.1)$$

$$\rho_1 = -8.933 \times T_1 + 4922 \text{ [kg/m}^3] \quad (A.2)$$

$$\sigma = 0.042705 \times \left[1.0 - \left(273.15 + \frac{T_1}{451.65}\right)\right]^{1.2532} \text{ [N/m]} \quad (A.3)$$

References

[1] T.G. Theofanous, J.P. Tu, A.T. Dinh, T.N. Dinh, The boiling crisis phenomenon part I: nucleation and nucleate boiling heat transfer, Exp. Therm. Fluid Sci. 26 (2002) 775–792.

[2] Y. Qi, J.F. Klausner, Comparison of gas nucleation and pool boiling site densities, J. Heat Transfer 128 (2005) 13–20.

[3] Y. Qi, J.F. Klausner, Heterogeneous nucleation with artificial cavities, J. Heat Transfer 127 (2005) 1189–1196.

[4] N.J. Nielsen, History of the inkjet printerhead development, HP J. 36 (1985) 4–10.

[5] Y. Iida, K. Okuyama, K. Sakurai, Boiling nucleation on a very small film heater subjected to extremely rapid heating, Int. J. Heat Mass Transfer 37 (1994) 2771–2780.

[6] L. Lin, A.P. Pisano, V.P. Carey, Thermal bubble formation on polysilicon micro resistors, J. Heat Transfer 120 (1998) 735–742.

[7] C.T. Avedisian, W.S. Osborne, F.D. McLeod, C.M. Curley, Measuring bubble nucleation temperature on the surface of a rapidly heated thermal inkjet heater immersed in a pool of water, Proc. R. Soc. Lond. A 455 (1999) 3875–3899.

[8] Z. Zhao, S. Glod, D. Poulikakos, Pressure and power generation during explosive vaporization on a thin-film microheater, Int. J. Heat Mass Transfer 43 (2000) 281–296.

[9] K.M. Balss, C.T. Avedisian, R.E. Cavicchi, M.J. Tarlov, Nanosecond imaging of microboiling behavior on pulsed-heated Au films modified with hydrophilic and hydrophobic self-assembled monolayers, Langmuir 21 (2005) 10459–10467.

[10] T. Rule, J. Kim, Heat transfer behavior on small horizontal heaters during pool boiling of FC-72, ASME J. Heat Transfer 121 (1999) 386–393.

[11] T. Chen, J.N. Chung, Coalescence of bubbles in nucleate boiling on microheaters, Int. Heat Mass Transfer 45 (2002) 2329–2341.

[12] S.J. Kline, F.A. McClintock, Describing uncertainties in single-sample experiments, Mech. Eng. 75 (1953) 3–8.

[13] V.P. Carey, Liquid–Vapor Phase Change Phenomena, Taylor and Francis, 1992, pp. 145–155.

[14] S. Kotake, I.I. Glass, Flows with nucleation and condensation, Prog. Aerospace Sci. 19 (1981) 129–196.

[15] M. Blander, J.L. Katz, Bubble nucleation in liquids, AIChE J. 21 (1975) 833–848.

[16] 3M Corporation, 3M Fluorinert Liquids Product and Contact Guide, 1995.

[17] V.P. Carey, A.P. Wemhoff, Thermodynamic analysis of near-wall effects on phase stability and homogeneous nucleation during rapid surface heating, Int. J. Heat Mass Transfer 48 (2005) 5431–5445.

[18] G.E. Thorncroft, J.F. Klausner, R. Mei, Bubble forces and detachment models, Multiphase Sci. Technol. 13 (3–4) (2001) 35–76.

[19] T. Chen, J.F. Klausner, J.N. Chung, Subcooled boiling heat transfer and dryout on a constant temperature microheater, Int. J. Heat Fluid Flow 25 (2004) 274–287.